Title
STRUCTURAL ANALYSIS OF SUPERCONDUCTING BENDING MAGNETS

Author
Meuser, R.B.

Publication Date
1980-05-01

Peer reviewed

MASTER

LBL-10950

CONF-800631--3

Lawrence Berkeley Laboratory
UNIVERSITY OF CALIFORNIA

Accelerator & Fusion Research Division

To be presented at the 8th International Cryogenic Engineering Conference, Genoa, Italy, June 3-6, 1980

STRUCTURAL ANALYSIS OF SUPERCONDUCTING BENDING MAGNETS

R. B. Meuser

May 1980

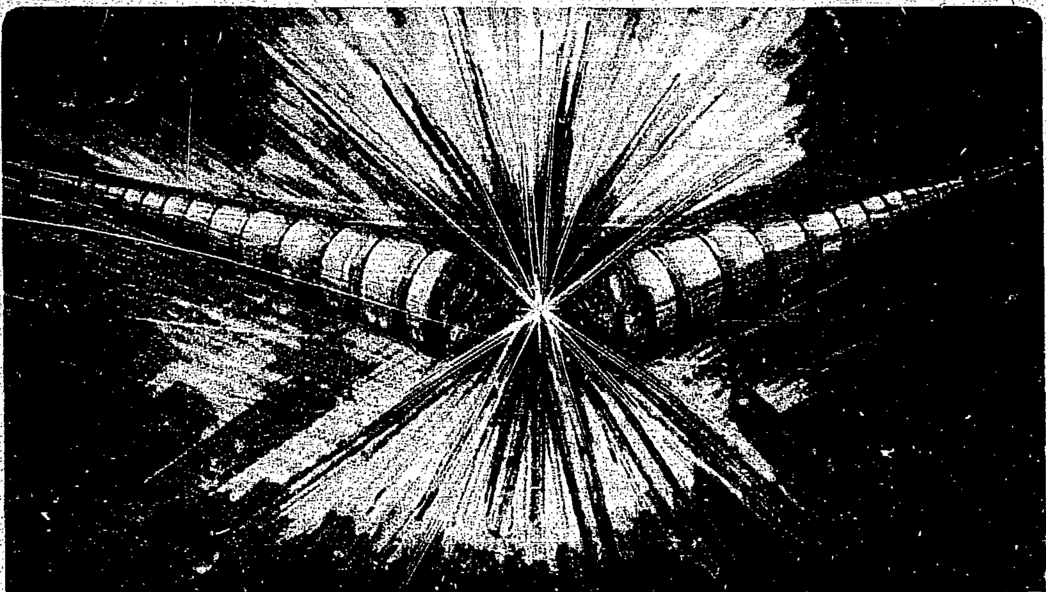

Prepared for the U.S. Department of Energy under Contract W-7405-ENG-48

STRUCTURAL ANALYSIS OF SUPERCONDUCTING BENDING MAGNETS

R. B. Meuser

Lawrence Berkeley Laboratory, Berkeley, California, U.S.A.

Mechanical stresses, displacements, and the effects of displacements upon aberrations of the magnetic field in the aperture have been calculated for a class of superconducting bending-magnet configurations. The analytical model employed for the coil is one in which elements are free to slide without restraint upon each other, and upon the surrounding structure. Coil configurations considered range from an idealized one in which the current density varies as cosine theta to more realistic ones consisting of regions of uniform current density. With few exceptions, the results for the more realistic coils closely match those of the cos θ coil.

INTRODUCTION

A superconducting bending magnet, or "dipole", intended for use in charged-particle accelerators and storage rings, usually consists of a winding in the form of a circular cylinder with longitudinal electric currents distributed so as to produce a uniform field in the region inside the winding (Fig. 1). The winding is surrounded by some sort of structure to resist the cumulative effects of the forces resulting from the interaction between the magnetic field and the electric currents -- the Lorentz body forces. The structure in turn is surrounded by an iron yoke.

To analyze the mechanics of the magnet coil, one must adopt some sort of "model" for a coil element. It is convenient to use the homogeneous, isotropic, linearly elastic model employed in the Theory of Elasticity because it approximates the conditions in many magnets. For idealized cases, useful analytical solutions have been obtained. For more complex coil configurations finite element analysis methods have been used.

However, for many magnets that we have built or plan to build at LBL, a far simpler model seems more appropriate. The model consists of conductor elements that are free to slide.(Fig. 2). Friction between elements, and between the coil and surrounding structure is ignored; we have little knowledge of the frictional properties of coil materials, especially after some 10^5 to 10^7 operating cycles.

Results are presented for the idealized "cosine theta" coil configuration and for a sampling of a broad spectrum of more realistic configurations that have been investigated. Also, some consideration of the mechanics of the restraining structure surrounding the coil is presented.

COIL STRESSES

We start with the simplest-possible coil model. In cross section, the coil is bounded by concentric circles, and the density of currents perpendicular to the section is $J = J_0 \cos \theta$, (A/m) independent of radius. (We call this the "idealized cosine-theta coil", and use the abbreviation "ICT coil" hereafter.)

To simplify things further initially, we assume the thickness of the coil to be small compared with its radius. We assume the circumferential stress is zero at the poles (θ = 90 deg.). If the stress is not zero, both the circumferential and radial stresses are increased by an additive constant.

For this thin ICT coil the field strength in the aperture (tesla) is (Fig. 3):

$$B_0 = (1/2)\ \mu_0\ J_0 h\ [1 + (a/b)^2]$$

The Lorentz body forces per unit (length x circum.)(N/m^2)are:

$$f_r = (1/4)\ \mu_0\ (J_0 h)^2\ a\ (a/b)^2\ (1 + \cos 2\theta)$$

$$f_t = -(1/4)\ \mu_0\ (J_0 h)^2\ a\ [1 + (a/b)^2]\ \sin 2\theta$$

The circumferential compressive pressure p_t and the radial pressure p_r acting outward (N/m^2) are:

$$p_r = (1/8)\ \mu_0\ (J_0 h)^2\ [1 + 3(a/b)^2](1 + \cos 2\theta)$$

$$p_t = (1/8)\ \mu_0\ (J_0 h)^2\ (a/h)\ [1 + (a/b)^2]\ (1 + \cos 2\theta)$$

Next we consider a thick ICT coil. The circumferential and radial pressures again vary as $1 + \cos\theta$. The thick-coil results are shown in Fig. 4 in comparison with those for the thin ICT coil of radius $a = (1/2)(a_1 + a_2)$ that produces the same aperture field. Fig. 4a shows how the total radial force at radius a_2 and the total circumferential force at $\theta = 0$ are affected by coil thickness and iron radius. Fig. 4b shows how the variation of circumferential stress through the thickness of the coil is affected by coil thickness and iron radius.

Two more realistic coils are represented in Figs. 1a and 1b. We will refer to these as the "layer-" and "block-type" coils, often referred to as "intersecting ellipse" and "cosine theta" coils respectively.

These two coil configurations have been analyzed for a wide range of parameters: One through three blocks or layers, coil radius ratios of 1.5 and 2.0, and for both close-fitting iron and no iron. The total radial and circumferential forces have been compared with those for thick ICT coils that produce the same aperture field. For the one-block or one-layer coils (which are identical), the differences are at most 15 percent. For two or more layers or blocks the differences are 7 percent or less.

The outside radial pressure distributions only roughly approximate those of the ICT coil. (Fig. 5). For the layer-type magnet, the circumferential stress (Fig. 6) in the innermost layers is substantially greater because those layers carry more current. For the block-type coils, the circumferential pressure distributions are indistinguishable from those for the equivalent ICT coils.

A third family of coils (Fig. 1c), which bear little resemblance to the ICT coil, has been investigated along with the surrounding ring structure. The distribution of circumferential stresses within each block is similar to that for the ICT coil. The radial forces are extremely irregular, of course, there being large concentrated loads at each wedge-shaped spacer. For only a single current "block", the total circumferential force is 20 to 25 percent lower than that for the equivalent thick ICT coil, depending on the iron radius; the maximum bending moment in the ring is 10 to 26 percent greater; the maximum displacement of the ring is 4 to 8 percent greater. These differences decrease rapidly as the number of blocks increases, all becoming less than 7 percent for three blocks.

SUPPORTING STRUCTURE

We present in turn: results for a thin, uniform, circular ring with the simplest possible radial load distribution; results for a thin ring with more complex loading, and results for a thick circular ring of uniform cross section with simple loading from an exact solution of the equations of the Theory of Elasticity.

The loading produced by an ICT coil is of the form $p = p_0 \cos 2\theta + p_1$ (N/m^2) The resulting internal forces and the displacements (Fig. 7) for a thin, uniform ring are:

Bending moment: $M = -(1/3)\ p_0\ a^2 \cos 2\theta$

Hoop tension: $T = -(1/3)\ p_0\ a \cos 2\theta + p_1\ a$

Radial shear: $V = (2/3)\ p_0\ a \sin 2\theta$

Radial displacement: $u = u_0 \cos 2\theta$, where $u_0 = p_0\ a^4/(9\ E\ I)$

Circumferential displacement: $v = -(u_0/2) \sin 2\theta$

M, T, and V are per unit axial length, with units N, N/m, and N/m respectively; a is the ring radius (m), I is the moment of inertia of the ring cross section per unit axial length (m^3), E is the elastic modulus (N/m^2).

But the loading produced by real coils is not the smooth loading produced by the ICT coil. To determine the effect of the irregularity of the loading, we considered the effect of a set of concentrated loads that approximate a continuous $1 + \cos 2\theta$ loading. For two loads, the maximum bending moment and displacement are 10 percent higher for the discontiuous loading than for the continuous one; each doubling of the number of loads reduces the difference by a factor of 1/4.

An exact solution of the equations of elasticity theory for a thick ring with surface pressure and shear forces is available. For a loading, $p = p_0 \cos 2\theta + p_1$ on the inside surface the relavent stresses and displacements are expressed by the following formulas:

$$\sigma_{t,in} = -\ 2\ K_1\ p_0\ (a_1/h)^2 \cos 2\theta + K_5\ p_1\ (a/h)$$

$$\sigma_{t,out} = +\ 2\ K_2 p_0\ (a_1/h)^2 \cos 2\theta + p_1\ (a/h)/K_6$$

$$\tau_{max} = K_3\ P_0\ (a_1/h) \sin 2\theta$$

$$u = \frac{4}{3} K_4 \frac{p_0\ a_1 (a_1/h)^3}{E} \cos 2\theta + K_7 \frac{p_1 a_1 (a/h)}{E}$$

$$v = -\frac{2}{3}\ K_4\ \frac{p_0\ a_1 (a/h)^3}{E} \sin 2\theta$$

The K-factors are presented in Fig. 8. Depending on the relative magnitudes of the p_0 and p_1 terms, the maximum circumferential stress can occur at either the inside or outside surface at either the $\theta = 0$ or 90 deg. positions.

CONCLUSIONS

With the exception of the circumferential stresses in the layer-type coils and the radial forces produced by the one-block coils, the stresses and displacements of the more realistic coils are closely approximated by those of the idealized cosine theta configuration. More complete results, including general multipole magnets and the effects of displacements upon field aberrations, are presented in Reference 1.

ACKNOWLEDGEMENTS

This work is supported by the office of High Energy and Nuclear Physics of the Department of Energy

REFERENCES

1. Meuser, R.B., Structural Analysis of Superconducting Multi-Pole Magnets, Report no. LBL-10940, Lawrence Berkeley Laboratory, Berkeley, CA, USA, 1980 (In process.)

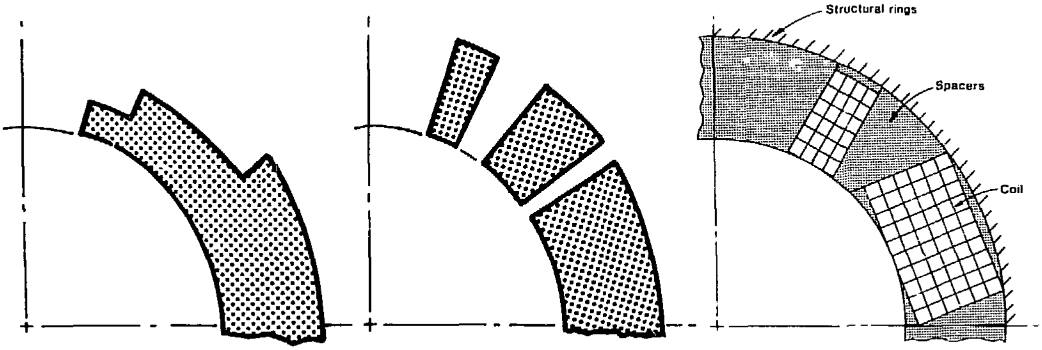

Fig. 1 Coil cross sections: (a) layer type; (b) block type; (c) rectangular-block type.

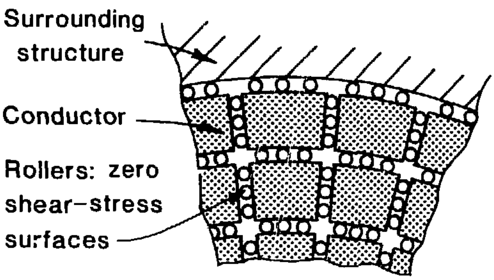

Fig. 2 Analytical model for coil structure.

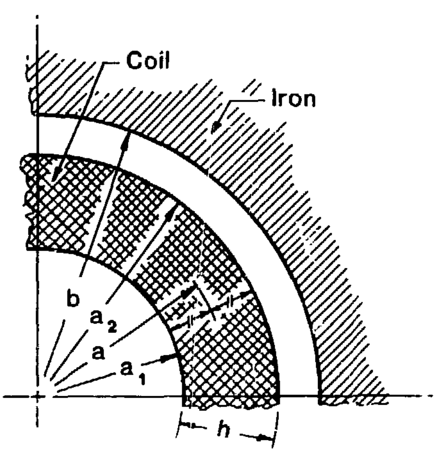

Fig. 3 Nomenclature for coils.

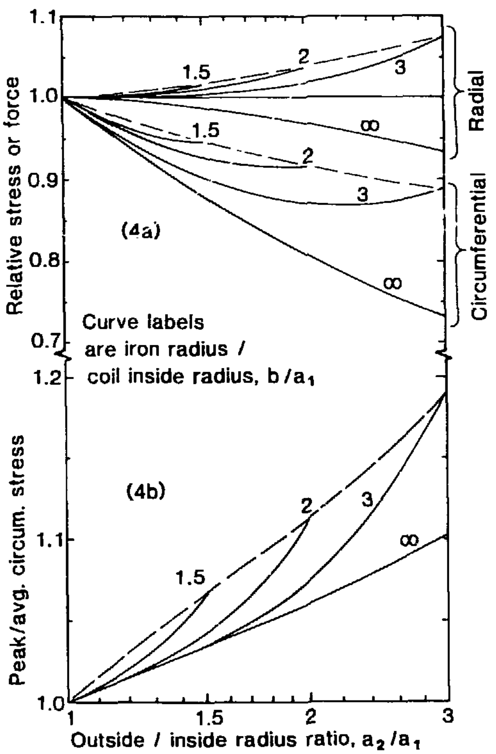

Fig. 4 Thick cos θ coil. Upper curves are max. radial stress on outside of coil and total circum. force normalized to values for thin coil producing same field. Lower curves are peak-to-average circum. stress ratio.

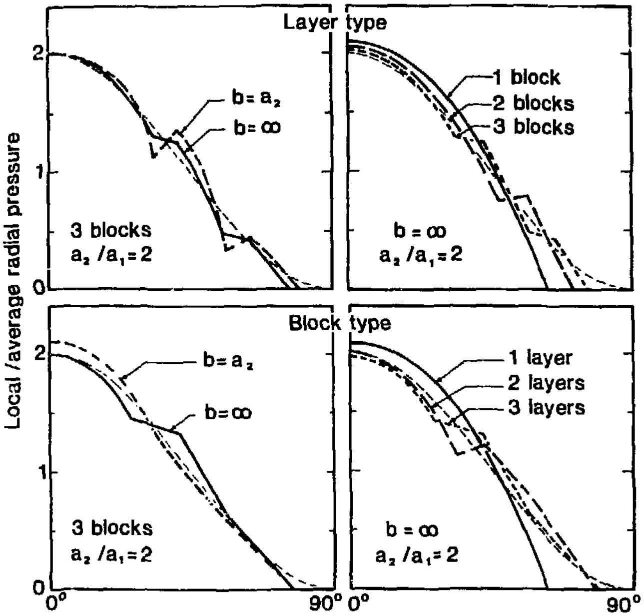

Fig. 5 Block- and layer-type coils; radial pressure distribution on outside: effects of iron radius, and number of blocks or layers.

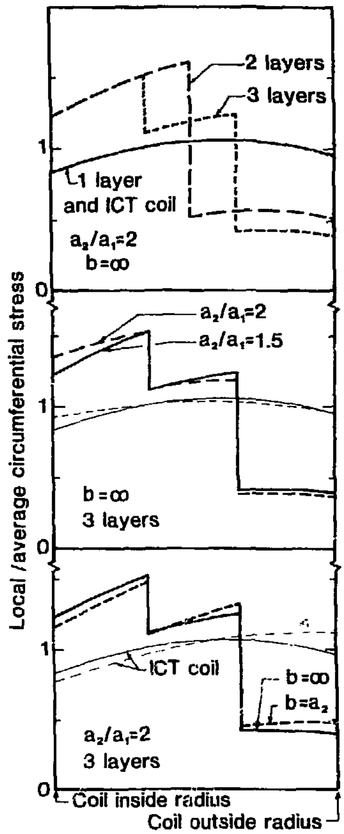

Fig. 6 Layer-type coils: circumferential stress distribution at θ = 0, effects of number of layers, coil thickness, and iron radius.

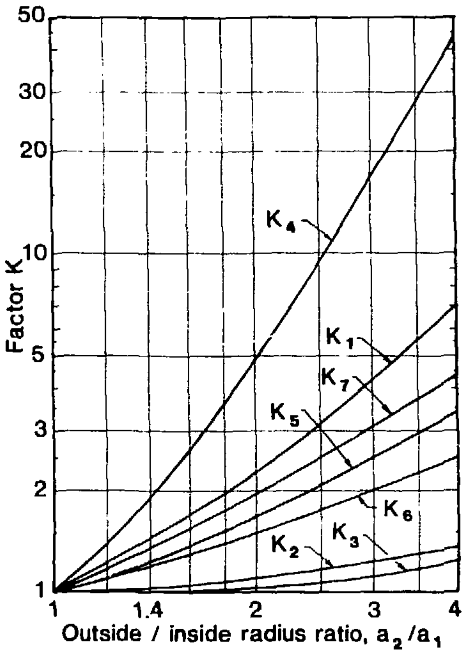

Fig. 8 Thick ring: factors for stresses and displacements.

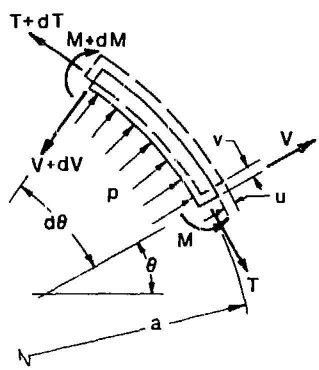

Fig. 7 Nomenclature for thin rings.